

# Reliability Assessment of Hydrofoil-Shaped Micro-Pin Fins

<sup>1</sup>David C. Woodrum, <sup>2</sup>Xuchen Zhang, <sup>1</sup>Peter A. Kottke,

<sup>1</sup>Yogendra K. Joshi, <sup>1</sup>Andrei G. Fedorov, <sup>2</sup>Muhannad S. Bakir, and <sup>1</sup>Suresh K. Sitaraman

<sup>1</sup>G. W. Woodruff School of Mechanical Engineering

<sup>2</sup>School of Electrical and Computer Engineering

Georgia Institute of Technology,

Atlanta, GA, 30332

Email: dwoodrum3@gatech.edu

## Abstract

As the need for high performance and extreme power dissipation microelectronic devices continues to rise, innovative thermal management solutions are being developed to efficiently remove the high heat fluxes dissipated in these applications. At heat flux rates surpassing the 1000 W/cm<sup>2</sup> level in some localized hot spot cases, conductive spreading to an external heat sink is no longer a viable thermal management option. On-chip, enhanced microfluidic cooling with pin fins offers new opportunities to deliver coolant in close proximity to power dissipation zones and hot spots. In state-of-the-art designs a two-phase refrigerant is pumped through a microfluidic channel within an active device absorbing heat at high velocity. Hydrofoil-shaped, silicon micro-pin fins populate the flow space to increase surface area available for heat removal and for liquid films to coalesce. The proposed thermal-management system has been fabricated by etching the microchannel with hydrofoil pin fins into the backside of the silicon device and then bonding it to a capping layer. While the hydrofoil shape is designed to benefit thermal-fluid performance properties, reliability consideration must also be given to the geometry. Phase change of the liquid facilitates optimal heat removal rates but also requires high-pressure conditions for operation. At these high-pressure conditions, the pin fins will be subjected to stress due to fluid pressure. Because of the unique geometry of the hydrofoil pin fins, special consideration must be given to the interaction of stress concentrations due to fluidic pressure loading and the small radius of curvature of the hydrofoil tail. The objective of this paper is to examine the various sources of stress in this high-performance, micro-pin fin channel and explore the reliability of this hydrofoil pin fin design under high-pressure conditions.

**Key Words:** reliability, microfluidic cooling, pin fin, stress concentration, two-phase flow

## Nomenclature

$\alpha$  the coefficient of thermal expansion (CTE)

$E$  modulus

$\nu$  Poisson's Ratio

## Introduction

The pursuit of higher performance computing necessitates denser and higher power microelectronics systems. As electrical systems produce greater and greater heat generation

rates in smaller, denser designs, new thermal management strategies must be developed to dissipate such large amounts of heat to maintain system performance. Traditional cooling techniques may no longer be effective for high heat generation rates in 100's of W/cm<sup>2</sup>. Such methods generally use a peripheral heat sink to drain heat from the source devices and reject it to an ambient fluid. This fluid is commonly the surrounding air or a liquid coolant within a flow loop. These approaches are effective for conventional microelectronics, but are limited by the thermal resistance between heat source and heat sink. [1]

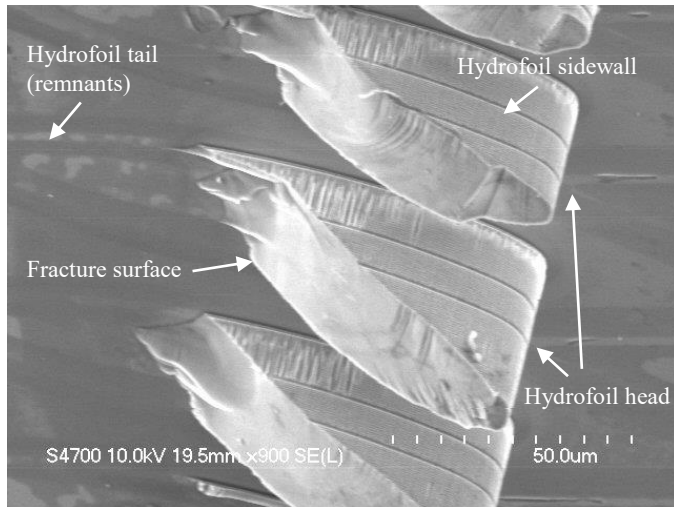
One approach in development at Georgia Tech utilizes on-chip cooling to actively cool the device. In this methodology, microchannels within or near the active devices are used to locally flow a coolant to remove high heat rates in close proximity to the sites of heat generation. The fluid is also maintained at saturated conditions for a portion of the flow domain; thus, as heat is absorbed, the fluid transitions from liquid to vapor. In this two-phase flow, a significantly larger energy reservoir is available to absorb heat due to the high latent heat of the coolant. This leads to much higher effective convection rates at the walls of the channel while also keeping the fluid temperature cooler as it passes through the heated zone [2]. In order to maintain the saturated conditions for fluid phase change, the fluid must be kept at high-pressure conditions for the expected operating temperatures. This pressure depends upon the fluid but can be on the order of 3000 kPa for some fluid choices [3].

The microchannel geometry itself also has key features which are necessary for heat transfer. The inclusion of micro-pin fins adds crucial surface area for heat transfer and sites for boiling to occur. In one design an array of 40 x 40 cylindrical pin fins having 100  $\mu$ m diameters populate the 1 cm x 1 cm square area of the microchannel. Such an array provides area enhancement, but also provides areas which are perpendicular to the flow direction and can even serve as structural support for the microchannel architecture. The natural improvement of such a system is to design the pin fins with a hydrofoil shape. This has numerous benefits including increasing the effective area for heat transfer further and reducing the pressure drop across the pin fins which decreases pumping power. [4]

As with any microelectronics design, special consideration must be given to any unique aspect which may adversely affect device reliability. In silicon devices such as this one, brittle fracture can occur under certain stress conditions ranging from 100 to 1000 MPa depending upon defect size

[5][6][7]. The high-pressure conditions inside of the device's microchannel raise questions regarding the limits on system performance. The hydrofoil pin fins present a possible threat to device reliability under such high-pressure conditions. Because of the natural shape of a hydrofoil which tapers a sharp point at the tail section, it is possible for stresses to concentrate on this tiny radius of curvature. This could lead to failures for even the most benign pressure loading conditions. Once a single feature fails, the neighboring structures are subjected to greater stress since the pressure loading remains constant. This could cause a series of rapid failures culminating in catastrophic failure, at which point the fluid escapes alleviating the internal pressure. In experiments, failures have occurred for internal fluid pressures on the order of 1 MPa. This fracture under monotonic loading could be due to a number of factors which include mechanical fracture of the hydrofoil pin fins. An example failure is shown in the SEM image of Figure 1. In this paper, fracture of the hydrofoil pin fin has been modeled and the results are summarized.

Fig. 1. SEM image of failed hydrofoil pin fins



## Device Fabrication

This design for on-chip cooling includes several key features. The microchannel itself incorporates hydrofoil pin fins, cylindrical support fins, flow stabilization fins, pressure taps, and inlet and outlet ports. These features are labeled in Figure 2. The hydrofoil pin fins serve to increase surface area and improve heat transfer. Larger cylindrical support pins help maintain device reliability under high-pressure conditions. Flow stabilization pins are required to mitigate transient effects within the two-phase flow. The pressure ports are necessary to evaluate the operating conditions of the fluid and to accurately determine the pressure within the channel at critical locations. To prevent leakage, a capping layer is required along with pristine bonding of the cap to the substrate. This experimental device is heated by platinum heaters which are patterned to carefully manage the allowable heat generation rates. All of these features are critical to device functionality and performance and require careful fabrication and processing.

During the fabrication process, SEM images are taken to verify dimensions and quality of etching. Figure 3 shows a top view of the fabricated microchannel with various features. For perspective, the features are also shown at an angle in an SEM image in Figure 4.

Fabrication of this design begins with a bare silicon wafer 500  $\mu$ m in thickness as shown in Figure 5. The silicon is etched to form the various features of the microchannel including the hydrofoil pin fins. Etch depths have ranged from 100 to 200  $\mu$ m depending on the design criteria. Functional heaters are deposited on the opposite side of the silicon substrate using chemical vapor deposition. The flow domain is then capped by a silicon cap which has the inlet and outlet ports etched through it. The two silicon masses are directly bonded to ensure sealing around the edges of the flow space.

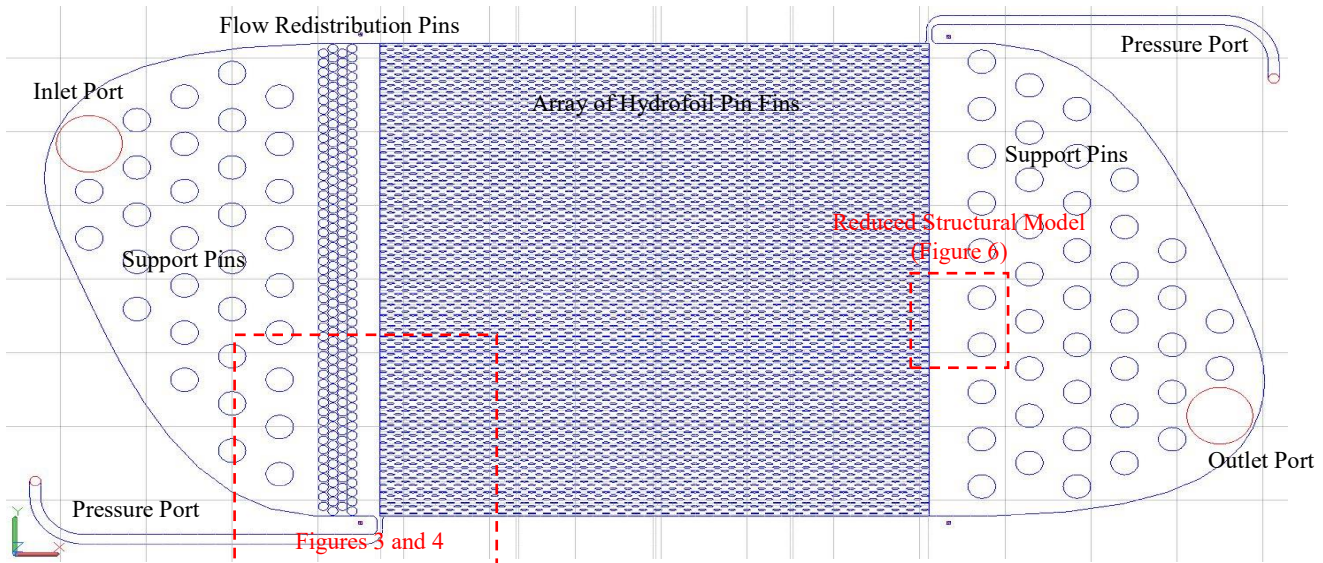


Fig. 2. Device Layout

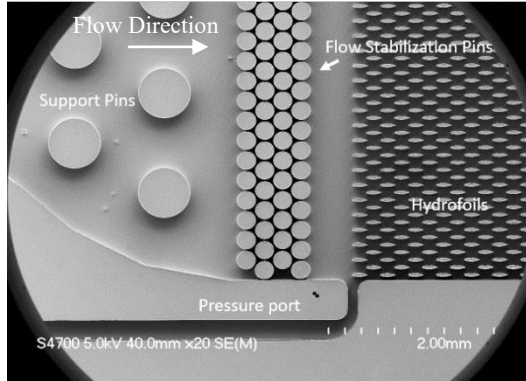


Fig. 3. SEM image of microchannel with relevant features

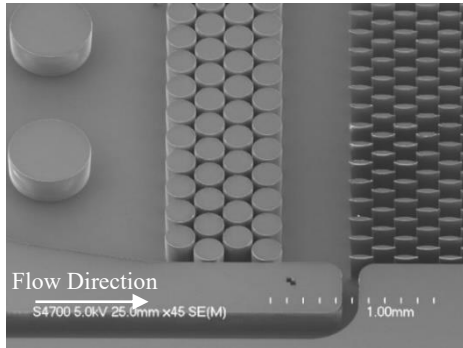


Fig. 4. Tilted view of etched pin fins

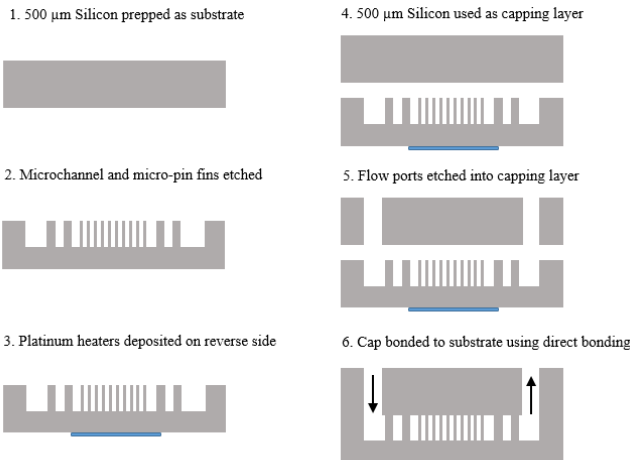


Fig. 5. Fabrication process flow diagram

### Structural Modeling

Based on this geometry and material set, mechanical modeling is conducted to determine the effect of fluid pressure on the hydrofoil pin fins. A 3-D structural model is developed through ANSYS® Mechanical. A simplified geometry is constructed which includes one column of hydrofoil pin fins and the adjacent support pins. This test section corresponds to the edge of the micro-pin fin array which is bordered by structural support pins. A view of the interior features of the model geometry is shown in Figure 6. This illustrates the

arrangement of pin fins beneath the silicon capping layer. As shown in Figure 7, the full system is loaded with an internal pressure and a cluster of nodes are constrained at one corner to prevent rigid body translation and rotation.

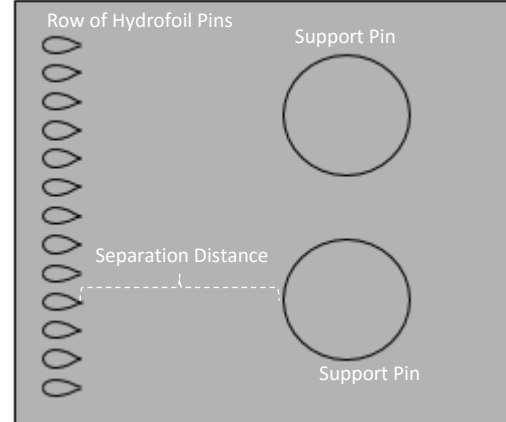


Fig. 6. Top view of the features of structural model

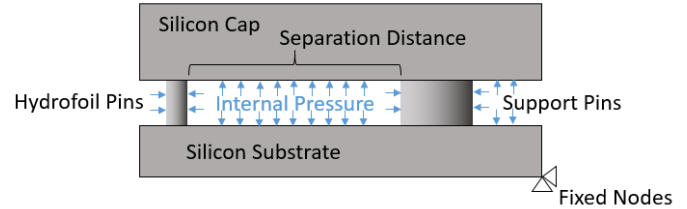


Fig. 7. Side view of structural model with boundary conditions

As seen in Figure 7, the internal pressure load is applied on all faces as in the closed system when fluid is exerting pressure on the walls. Experimental failures are observed for pressures in excess of 1 MPa, and thus this is the loading condition of interest. Once again such high pressures are required for achieving saturated conditions at the expected temperature of operation. This allows for the fluid to change phase, further increasing the rates of heat removal. A static uniform pressure across the system is not identical to operating conditions since the pressure must drop from inlet to outlet due to fluid flow, but assuming a uniform pressure in the model is a worst case scenario as the pressure assumed is the maximum pressure experienced anywhere within the microchannel during operation. The necessary material properties for silicon are shown in Table 1 [8]. All geometric values not previously addressed are shown in Table 2.

TABLE 1: MATERIAL PROPERTIES

Parameter	Silicon
Material Model	Elastic Anisotropic
Modulus, E	$C_{11}: 166 \text{ GPa}$ $C_{12}: 63 \text{ GPa}$ $C_{44}: 80 \text{ GPa}$
Poisson, $\nu$	0.28

TABLE 2: GEOMETRIC PARAMETERS

Parameter	Value
Width/Length Model	3 mm
Diameter Support	500 $\mu\text{m}$
Length Hydrofoil	100 $\mu\text{m}$
Width Hydrofoil	40 $\mu\text{m}$
Pitch Hydrofoil	100 $\mu\text{m}$
Height Microchannel	200 $\mu\text{m}$
Separation Distance	1000 $\mu\text{m}$

The size of the mesh elements positioned within or near the hydrofoil features is critical, as this is the expected zone of high stress. Consideration is given to properly size the elements for shape while maintaining reasonable calculation times. The full geometry with this mesh sizing is shown in Figure 8. In using the anisotropic material properties for silicon, the mesh assumes the highest stiffness to be in the x-direction.

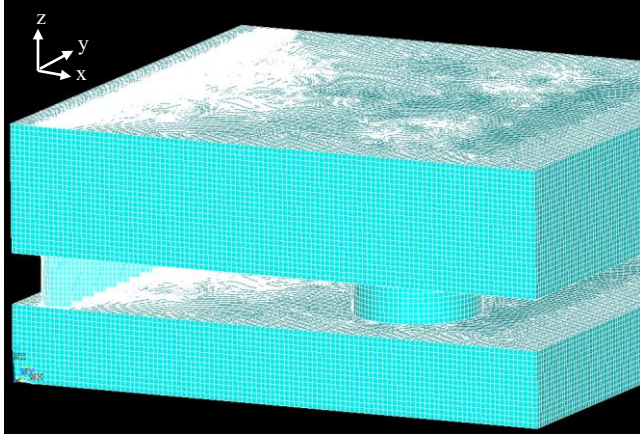


Fig. 8. Mesh of full geometry with 5  $\mu\text{m}$  mesh size for hydrofoil pins

### Structural Results

The model is built according to this geometric and material layout and loaded with the boundary conditions discussed. The system is solved to determine the stress distribution within the microchannel architecture. For the stress results shown in Figure 9, the system is loaded with a uniform pressure of 1 MPa. The results indicated are for first principal stress values as silicon is a brittle material expected to fail based on this criterion. The model deformation is included visually but is exaggerated. The over-pronounced bulging of the unconstrained zone demonstrates how this section bends due to applied pressure.

The resulting stress field indicates stress concentrations at the tail of the hydrofoil pin fins as well as on the outer surface of the support pins. These are the solid features nearest to the unconstrained zone; thus, these features must accept a majority of the pressure loading acting on the exposed faces of the unconstrained zone. Due to the relatively large separation distance between the hydrofoil pins and the support pins, the

pressure acting on the unconstrained zone creates a large moment arm leading to high stress on these pin features.

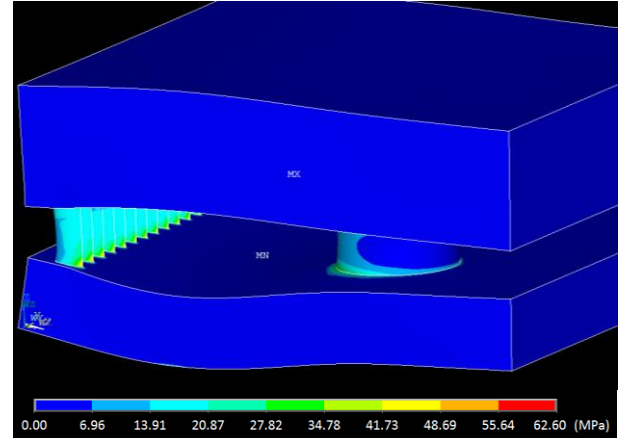


Fig. 9. First principal stress results for 1 MPa pressure loading (Deformation is exaggerated.)

Similar to a plate with a uniformly distributed load over its surface and supported by few columns at varying distances from one another, this situation illustrates how the separation distance acts to amplify the stress at the concentration point as the plate flexes. In this case the hydrofoil tail is subjected to an even higher stress concentration as the geometry of the tail tapers down. This concentration is shown in Figure 10. For the coarse mesh size in this case (5  $\mu\text{m}$ ) the maximum stress at one of these tail concentrations is approximately 63 MPa. Since this tail is a sharp corner, the resulting stress depends upon mesh size, but converges for mesh sizes less than 5  $\mu\text{m}$  as shown by the blue markers in Figure 12.

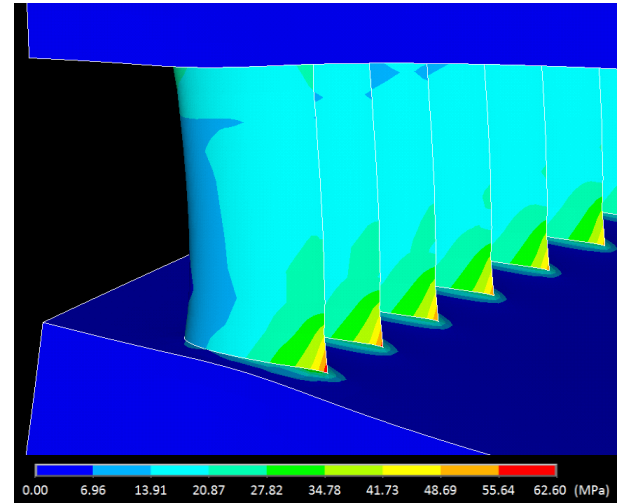


Fig. 10. Zoomed view of stress concentration on hydrofoil fin

As an exploratory technique, the same structural modeling is conducted on a “smoothed” hydrofoil geometry. This shape, shown in Figure 11 alongside the standard geometry, retains the head of the hydrofoil geometry but allows for a significant reduction in the sharpness of the downstream “tail” end of the pin fin. The pin-fin cross section is truncated by an arc of radius 20  $\mu\text{m}$  which serves to better distribute the stress received from the “unconstrained zone.”

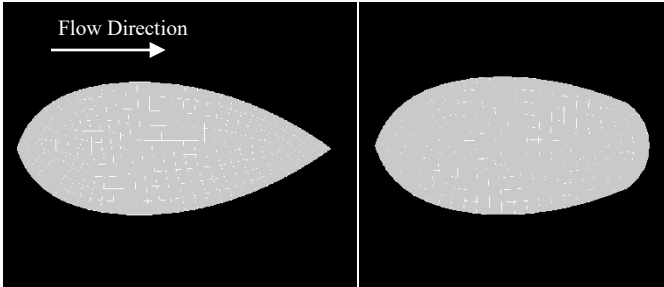


Fig. 11. Comparison of model hydrofoil shapes for 5  $\mu\text{m}$  mesh size (left: standard, right: smoothed)

The same modeling procedure is utilized for the smoothed hydrofoil geometry resulting in a decrease in the maximum stress within the pin fins for most mesh sizes. A mesh convergence is conducted by locally increasing the mesh density in and around the hydrofoil pin fins for both standard and smoothed cases. This comparison is shown in Figure 12. The stress does in fact continue to increase as mesh density increases, but once the mesh size is below 10  $\mu\text{m}$ , the error is less than 10% from iteration to iteration, indicating the stress values are relatively accurate near a mesh size of 5  $\mu\text{m}$ .

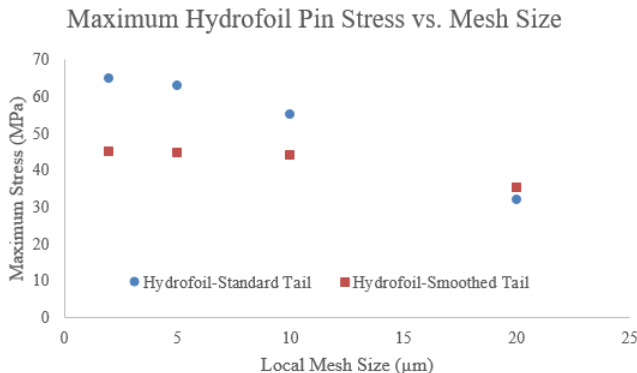


Fig. 12. Mesh convergence study for structural model

Qualitatively, the resulting stress due to pressure loading is more evenly distributed across the smoothed pin fins compared to the sharp tail end of the standard hydrofoil pin fins. This results in a 35 percent decrease in the stress experienced by the hydrofoil features from 65 MPa to 42 MPa for the smoothed feature design. This reduction in stress in the smoothed design theoretically allows for higher operating pressures to be tolerated before failure when compared against the standard hydrofoil pin design.

In addition to exploring the effects of pin shape on stress, a study is conducted to determine the effect that the separation distance between the hydrofoil pins and the adjacent support structures has on the maximum stress experienced by the pins. The separation distance between large support pin and the row of hydrofoil pins (indicated in Figures 6 and 7) is originally assumed to be 1000  $\mu\text{m}$ . In this parametric study the separation distance varies from 250 to 1000  $\mu\text{m}$ . The model geometry is augmented for the new separation distance and solved to determine the maximum principal stress. For each value of separation distance, the mesh size used for the hydrofoil pins is maintained at a constant value of 10  $\mu\text{m}$  as to

avoid unwanted mesh size effects which could cause discrepancies in the relative comparison of stress across the study. The results for the four different separation distances are shown in Figure 13.

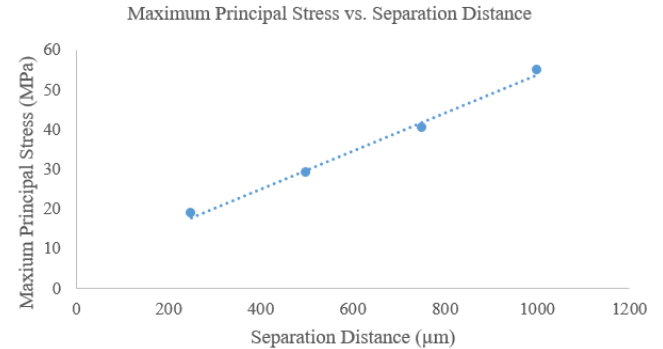


Fig. 13. Plot of maximum stress vs. separation distance with linear fit line

For each incremental decrease (250  $\mu\text{m}$  increments) in separation distance from the original 1000  $\mu\text{m}$  the maximum principal stress experienced by the silicon model is also reduced. For this set of model results at constant mesh size, the relationship between separation distance and maximum stress has a linear correlation coefficient greater than 0.99. While reducing the feature separation distance could theoretically increase tolerable pressures by a large factor, this imposes larger pressure drops and restricts flow as the number of supports goes up. Both mechanical and fluidic aspects of device performance must be considered during the design process to ensure acceptable overall system operation.

In order to decrease the propensity for failure in future system designs, attention should be given to the radius of curvature of the hydrofoil. Specifically, augmenting the radius of the hydrofoil tail reduces the magnitude of the stress concentration that occurs at this location. The limits of fabrication resolution should also be considered to ensure that the radius of sharp features is known for all possible stress concentration locations. Another approach to mitigate failures would be to increase the number and density of the support structures. By reducing the separation distance between support and the hydrofoil pins, the magnitude of the stress concentration will be reduced. While changing the hydrofoil shape and spacing would augment the mechanical performance of the system, these changes would also affect the thermal and fluidic performance specifications of the design. In this way the layout of the microchannel features directly impacts thermal, fluidic, and mechanical performance of the device.

## Conclusion

This paper presents an emerging technology for next generation microelectronics cooling, along with the fabrication process for this design. Reliability concerns related to the hydrofoil pin fins and their unique geometry are discussed. During operation the solid surfaces are expected to be subjected to pressures in excess of 500 kPa. The loading case of 1 MPa is considered since experimental failures are observed for this condition. A structural model is developed to

explore the stress field resulting from fluidic pressures within the microchannel architecture. Based on this structural model the first principal stresses are shown to range up to 65 MPa. The hydrofoil pin fin experiences a stress concentration on the sharp radius of curvature of the hydrofoil tail. Because of this concentration, failures may be expected to occur for reduced loading conditions compared to designs which do not utilize hydrofoil pin fins. An improved design for the hydrofoil geometry is tested via the same modeling scheme. By reducing the sharpness of the hydrofoil tail, the resulting principal stress is shown to be reduced to approximately 42 MPa. Mitigation strategies for a redesign of this system are discussed which include this blunting of the hydrofoil tail curvature as well as populating the flow domain with additional supports to reduce stress for a given loading condition. The effect of separation distance on stress within the modeling framework is presented, and a strong linear correlation is demonstrated. The modeling and results presented in this paper emphasize the need for co-design when engineering a microelectronics architecture, particularly the inclusion of mechanical modeling alongside the electrical, thermal, and fluidic disciplines.

### Acknowledgments

The authors acknowledge DARPA ICECool Fundamentals and Applications Programs for support of this work under contract numbers W31P4Q-12-1-0014 and HR0011-14-1-0002, respectively.

### References

- [1] Lasance, C., Simons, R.E., Advances in high-performance cooling for electronics, *Electronics Cooling*, (2005), pp. 11.
- [2] Y. Peles, Two-phase boiling flow in microchannels-instabilities issues and flow regime mapping, in: 1st International Conference on Microchannels and Minichannels, ASME, New York, NY, 2003, pp. 559–566.
- [3] Kottke, P. A., Yun, T. M., Green, C., Joshi, Y. K. and Fedorov, A. G., Two-phase convective cooling for ultra-high power dissipation in microprocessors, *ASME J. Heat Transfer*, 138 (1), 011501-011507 (2015).
- [4] A. Bar-Cohen, et al., “Two-phase thermal transport in microgap channels—theory, experimental results, and predictive relations,” *Microgravity Science and Technology* vol. 24, no. 1, pp. 1-15, Jan. 2012.
- [5] Chong, D.Y.R.; Lee, W.E.; Lim, B.K.; Pang, John H.L.; Low, T.H., "Mechanical characterization in failure strength of silicon dice," in *Thermal and Thermomechanical Phenomena in Electronic Systems*, 2004. IITHERM '04. The Ninth Intersociety Conference on, vol.2, no., pp.203-210 Vol.2, 1-4 June 2004
- [6] V. Hatty, et al., “Fracture toughness, fracture strength, and stress corrosion cracking of silicon dioxide thin films,” *J. Microelectromechanical Systems*, vol.17, no.4, pp. 943-947, Aug. 2008
- [7] Woodrum, D.C.; Sarvey, T.; Bakir, M.S.; Sitaraman, S.K., “Reliability study of micro-pin fin array for on-chip cooling,” in *Electronic Components and Technology Conference (ECTC) , 2015 IEEE 65th* , vol., no., pp.2283-2287, 26-29 May 2015
- [8] J. J. Wortman and R. A. Evans, “Young’s modulus, shear modulus, and Poisson’s ratio in silicon and germanium”, *J. Applied Physics*, vol. 36(1), pp. 153–156, Jan. 1965.
- [9] S. Michaelides and S. K. Sitaraman, “Die cracking and reliable die design for flip-chip assemblies,” *IEEE Trans. Adv. Packag.*, vol. 22, pp. 602–613, Nov. 1999.